Electronic Research Archive

https://www.aimspress.com/journal/era

ERA, 34(10): 7244–7260.
DOI: 10.3934/era.2026313
Received: 09 July 2026
Revised: 02 August 2026
Accepted: 06 August 2026
Published: 19 August 2026

Theory article

Exponential synchronization of reaction-diffusion neural networks via asynchronous sampled-data event-triggered control

Pingge Chen, Haibo Zeng and Chenjie Xu*

College of Science, Hunan University of Technology, Zhuzhou 412007, China

* **Correspondence:** Email: xu-chengjie@163.com.

Abstract: This paper investigated the exponential synchronization (ES) problem of reaction-diffusion neural networks over directed networks under an asynchronous sampled-data event-triggered intermittent control scheme. By integrating event-triggered communication and intermittent control mechanisms, hybrid control framework was developed to reduce communication transmissions and control activation time. A Lyapunov–Krasovskii functional (LKF) involving historical-state integral terms was constructed, and sufficient synchronization conditions were derived using graph-theoretic techniques and inequality methods. The proposed criterion guaranteed exponential convergence of synchronization errors and avoided Zeno behavior. Numerical simulations demonstrated that the proposed strategy achieved satisfactory synchronization performance with reduced communication requirements.

Keywords: reaction-diffusion neural networks; exponential synchronization; sampled-data control; intermittent control; event-triggered control; directed networks

1. Introduction

Reaction-diffusion neural networks (RDNNs) have attracted increasing attention in the study of complex dynamical systems and networked control problems [1]. As an important collective behavior in networked systems, synchronization has been widely studied because of its significant applications in secure communication, distributed control, and signal processing. Dimarogonas et al. [2] investigated distributed event-triggered control for multi-agent systems and developed communication-efficient control strategies. Girard [3] proposed dynamic triggering mechanisms to reduce unnecessary transmissions while maintaining system performance. Lu [4] studied synchronization-related stability problems of reaction-diffusion neural networks and established sufficient stability conditions.

However, with the increasing complexity and scale of networked systems, reducing communication consumption and control costs while maintaining synchronization performance remains a challenging problem [5].

To address resource limitations in networked systems, event-triggered control (ETC) and intermittent control have been widely investigated. Wu et al. [6] studied intermittent control strategies for fixed-time synchronization of coupled networks. Huang et al. [7] investigated event-triggered passivity of delayed reaction-diffusion memristive neural networks with fixed and switching topologies. Zhang et al. [8] proposed a monotonically increasing function-based event-triggered sampling scheme for networked nonlinear systems. Zhang et al. [9] developed an accumulated-state-error-based triggering strategy for sampled-data systems. Meanwhile, Huang et al. [10] and Lin et al. [11] further investigated synchronization and passivity problems of neural networks under event-triggered communication and intermittent control mechanisms. Ma et al. [12] further studied synchronization control of chaotic neural networks subject to actuator saturation under an event-triggered sampling scheme. These methods provide effective approaches for reducing communication burden and energy consumption in synchronization control problems.

Despite these achievements, the integration of event-triggered communication and intermittent control for reaction-diffusion neural networks remains limited. Existing results mainly focus on reducing communication frequency or controller activation time separately. For instance, Qiu and Su [13] investigated sampled-data event-triggered synchronization of reaction-diffusion neural networks to reduce communication consumption, while Liu et al. [14] developed an asynchronous intermittent control approach to reduce controller activation time. However, the exponential synchronization (ES) problem of reaction-diffusion neural networks over directed networks under a sampled-data event-triggered asynchronous aperiodic intermittent control scheme has not been fully investigated.

Motivated by the above observations, this paper investigates the ES problem of reaction-diffusion neural networks over directed networks under a sampled-data event-triggered asynchronous aperiodic intermittent control scheme. By integrating event-triggered communication and intermittent control, a hybrid control scheme is proposed to simultaneously reduce communication transmissions and controller activation time. The main contributions are summarized as follows.

1) A sampled-data event-triggered asynchronous aperiodic intermittent control scheme is developed for reaction-diffusion neural networks over directed networks. Unlike existing methods that separately consider communication reduction or intermittent control, the proposed scheme combines both mechanisms to achieve ES with reduced resource consumption.

2) An Lyapunov–Krasovskii functional (LKF) with historical-state integral terms is constructed to characterize the effects of sampled-data communication and asynchronous intermittent control. Based on this functional, sufficient conditions for ES are derived by employing graph-theoretic techniques and inequality methods.

3) The proposed event-triggering mechanism is proved to be Zeno-free. Numerical simulations are provided to verify the effectiveness of the proposed control scheme.

The remainder of this paper is organized as follows. Section 2 introduces the system model, assumptions, and control protocol. Section 3 presents the synchronization criteria and theoretical analysis. Section 4 provides numerical examples. Finally, Section 5 concludes this paper.

2. Preliminaries and description model

2.1. Notations

Consider a collection of nodes represented by $\mathcal{N} = \{1, 2, \ldots, N\}$. Let $\mathbb{R}^n$ denote the n-dimensional Euclidean space and define $\mathbb{R}^+ = [0, +\infty)$. Denote by $C^{2,1}(\mathbb{R}^n \times \mathbb{R}^+; \mathbb{R}^+)$ the class of nonnegative functions $U(s,t)$ on $\mathbb{R}^n \times \mathbb{R}^+$ that are twice continuously differentiable with respect to s and continuously differentiable with respect to t. For a vector-valued function $x(s,t) \in \mathbb{R}^n$, the notation $\|x(s,t)\|_2$ denotes the Euclidean norm with respect to the state vector, $\|x(s,t)\|_2 = \left(\sum_{k=1}^{n} x_k^2(s,t)\right)^{1/2}$, where $s \in \Gamma$ is the spatial variable. Throughout this paper, the spatial energy of the state is measured by the L^2-norm $\int_\Gamma \|x(s,t)\|_2^2 \mathrm{d}s$. Let $\Gamma \subset \mathbb{R}^k$ be a bounded compact domain satisfying $\mathrm{mes}(\Gamma) > 0$. Moreover, $\phi(s) \in C^1(\Gamma)$ means that $\phi(s)$ possesses a continuous first-order derivative throughout the domain Γ.

A directed graph (digraph) is represented by $\mathcal{G} = (\mathcal{N}, E)$, where $\mathcal{N}$ is the vertex set and E is the set of directed edges. Two weighted adjacency matrices, $A = (a_{ij}), B = (b_{ij})$, are introduced in this paper. Matrix A characterizes the coupling topology of the reaction-diffusion neural network, whereas matrix B is associated with the distributed controller. Accordingly, $a_{ij} > 0$ (or $b_{ij} > 0$) if node j can directly transmit information to node i; otherwise, $a_{ij} = 0$ (or $b_{ij} = 0$).

Throughout this paper, $z_i(s,t)$ and $w_i(s,t)$ denote the states of the drive system and the response system, respectively. The synchronization error is defined as $v_i(s,t) = w_i(s,t) - z_i(s,t)$. Moreover, $\tilde{z}_i(s,t)$ denotes the sampled state used in the event-triggered controller, which is updated only at the corresponding triggering instants.

2.2. Mathematical model

This paper considers the ES problem of reaction-diffusion neural networks under asynchronous aperiodic intermittent control.The interactions among the nodes are characterized by a directed graph $\mathcal{G}$ with $N(N \geq 2)$nodes, and the network dynamics are formulated as

$$\frac{\partial z_i}{\partial t} = \sum_{o=1}^{K} \frac{\partial}{\partial s_o}\left(B_{io}\frac{\partial z_i}{\partial s_o}\right) + f_i(z_i) + \sum_{j=1}^{N} a_{ij}H_{ij}(z_i, z_j), i \in \mathcal{N} \tag{2.1}$$

The vector $z_i(s,t)$ denotes the state of the ith node of the network, where t denotes the time variable and $s = (s_1, s_2, \ldots, s_k) \in \Gamma \subset \mathbb{R}^k$ represents the spatial variable. The spatial domain is defined by $\Gamma = \{s = (s_1, s_2, \ldots, s_k)^{\mathrm{T}} \mid \|s_i\|_2 < n_i,\ n_i > 0,\ i = 1, 2, \ldots, k\}$, which is a bounded compact subset of $\mathbb{R}^k$ satisfying $\mathrm{mes}(\Gamma) > 0$. The activation function $f_i(\cdot) : \mathbb{R}^m \to \mathbb{R}^m$ is assumed to be continuous. Moreover, $B_{io} > 0$ denotes the diffusion coefficient corresponding to the i-th node. The interconnection among different nodes is described by the coupling function $H_{ij}(\cdot,\cdot) : \mathbb{R}^m \times \mathbb{R}^m \to \mathbb{R}^m$ together with the coupling weight a_{ij}.

System (2.1) is subject to the following initial state and boundary conditions:

$$z_i(s,t) = 0, \quad (s,t) \in \partial\Gamma \times [0, +\infty) \tag{2.2}$$

$$z_i(s,0) = \phi_i(s,0), \quad s \in \Gamma, \quad i \in \mathcal{N} \tag{2.3}$$

The boundary condition (2.2) is the homogeneous Dirichlet boundary condition, which requires the state variables to vanish on the boundary of the spatial domain. The same boundary condition is imposed on both the drive and response systems throughout this paper.

Assume that $\phi(s,0) = (\phi_1^{\mathrm{T}}(s,0), \phi_2^{\mathrm{T}}(s,0), \ldots, \phi_N^{\mathrm{T}}(s,0))^{\mathrm{T}}$ is a bounded and continuous initial condition on Γ. On the basis of System (1), the following response system is constructed:

$$\frac{\partial w_i}{\partial t} = \sum_{o=1}^{K} \frac{\partial}{\partial s_o}\left(B_{io}\frac{\partial w_i}{\partial s_o}\right) + f_i(w_i) + \sum_{j=1}^{N} a_{ij}H_{ij}(w_i, w_j) + u_i, \quad i \in \mathcal{N} \tag{2.4}$$

where $w_i(s,t)$ corresponds to the state variable and u_i to the control input.

$$w_i(s,t) = 0, \quad (s,t) \in \partial\Gamma \times [0, +\infty) \tag{2.5}$$

$$w_i(s,0) = \phi_i(s,0), \quad s \in \Gamma, \quad i \in \mathcal{N} \tag{2.6}$$

In the above system, $w_i(s,t)$ represents an m-dimensional state vector. The control goal is to achieve ES between Systems (2.1) and (2.4).

The synchronization error is defined as $v_i = v_i(s,t) = w_i(s,t) - z_i(s,t)$, and the error states satisfy the following formula:

$$\frac{\partial v_i}{\partial t} = \sum_{o=1}^{K} \frac{\partial}{\partial s_o}\left(B_{io}\frac{\partial v_i}{\partial s_o}\right) + (f_i(w_i) - f_i(z_i)) + \sum_{j=1}^{N} a_{ij}(H_{ij}(w_i, w_j) - H_{ij}(z_i, z_j)) + u_i, \quad i \in \mathcal{N} \tag{2.7}$$

Correspondingly, the error system satisfies the same boundary conditions.

A conventional distributed controller is considered as $u_i(s,t) = \alpha \sum_{j \in \mathcal{N}_i} b_{ij}(z_i(s,t) - z_j(s,t))$, where b_{ij} denotes the (i,j)-th entry of the weighted adjacency matrix B, $\mathcal{N}_i$ represents the neighbor set of node i, and α is the coupling strength.

This controller requires continuous state information exchange among neighboring nodes, resulting in high communication frequency. To reduce communication requirements, continuous states are replaced by sampled states, and the following sampled-data event-triggered controller is adopted:

$$u_i(s,t) = \alpha \sum_{j \in \mathcal{N}_i} b_{ij}(\tilde{z}_i(s, t_r^i) - \tilde{z}_j(s, t_{r'}^j)), \quad t \in [t_r^i, t_{r+1}^i).$$

Here, $\tilde{z}_i(s, t_r^i)$ denotes the latest sampled state of node i, and $\tilde{z}_j(s, t_{r'}^j)$ represents the latest available sampled state of node j. Since each node determines its triggering instants independently, r' is generally different from r, which characterizes the asynchronous property of the proposed controller. Communication delays are neglected, and all nodes use the same sampling period for event detection.

For each node $i \in \mathcal{N}$, the sequence t_r^i ($r \in \mathcal{N}$) represents its event-triggering instants, with $t_0^i = 0$ as the initial triggering time. In addition, h is the corresponding sampling period.

$$t_{r'}^j = \max\left\{ t_q^j \middle| t_q^j \le t_r^i + lh, q \in \mathcal{N}, l \in \mathcal{N}^+ \right\}. \tag{2.8}$$

Suppose that $t_r^i + lh$ represents the current sampling instant. Then, the triggering error signals for the i-th and j-th nodes can be expressed, respectively, as

$$e_i(s, t_r^i + lh) = \tilde{z}_i(s, t_r^i) - \tilde{z}_i(s, t_r^i + lh) \tag{2.9}$$

$$e_j(s, t_r^i + lh) = \tilde{z}_j(s, t_{r'}^j) - \tilde{z}_j(s, t_r^i + lh) \tag{2.10}$$

$$e_i(s,rh) = v_i(s,t_r^i) - v_i(s,rh) = -\int_{t_r^i}^{rh} \frac{\partial v_i(s,\tau)}{\partial \tau} \mathrm{d}\tau. \tag{2.11}$$

where e_i and e_j represent the triggering errors of node i and j, respectively. For any $t \in [t_r^i + lh, t_r^i + lh + h)$, the following relation holds:

$$\begin{aligned} \tilde{z}_i(s,t_r^i) - \tilde{z}_j(s,t_{r'}^j) &= [\tilde{z}_i(s,t_r^i) - \tilde{z}_i(s,t_r^i + lh)] + [\tilde{z}_i(s,t_r^i + lh) - \tilde{z}_j(s,t_r^i + lh)] + [\tilde{z}_j(s,t_r^i + lh) - \tilde{z}_j(s,t_{r'}^j)] \\ &= e_i(s,t_r^i + lh) - e_j(s,t_r^i + lh) + [\tilde{z}_i(s,t_r^i + lh) - \tilde{z}_j(s,t_r^i + lh)] \end{aligned} \tag{2.12}$$

Consequently, for any $t \in [rh, (r+1)h)$, the following relation holds:

$$u_i(s,t) = \alpha \sum_{j \in \mathcal{N}_i} b_{ij}(e_i(s,rh) - e_j(s,rh) + z_i(s,rh) - \tilde{z}_j(s,rh)) \tag{2.13}$$

The sequence of triggering instants is generated recursively through:

$$t_{r+1}^i = t_r^i + \min_{l \geq 1} \left\{ lh : \|e_i(s,t_r^i + lh)\|_2 > \varphi_i \sum_{j \in \mathcal{N}_i} b_{ij} \|\tilde{z}_i(s,t_r^i) - \tilde{z}_j(s,t_{r'}^j)\|_2 \right\}. \tag{2.14}$$

where φ_i is a positive constant that will be chosen appropriately.

Remark 1. The proposed sampled-data event-triggered asynchronous aperiodic intermittent control scheme integrates communication scheduling and control activation. The triggering parameter φ_i establishes a trade-off between communication efficiency and synchronization performance. Specifically, a smaller φ_i induces more frequent triggering, whereas a larger φ_i reduces communication transmissions.

Definition 2.1 [2]: The closed-loop system is regarded as Zeno-free if the inter-event intervals fulfill

$$\inf_{r \in \mathcal{N}} \left(t_{r+1}^i - t_r^i \right) > 0, \quad \forall i \in \mathcal{N}.$$

Remark 2. It follows from (2.14) that the event-triggering mechanism is evaluated only at the sampling instants. Whenever the inequality

$$\|e_i(s,t_r^i + lh)\|_2 > \varphi_i \sum_{j \in \mathcal{N}_i} b_{ij} \left\| \tilde{z}_i(s,t_r^i) - \tilde{z}_j(s,t_r^j) \right\|_2$$

holds, node i generates a triggering event at $t_r^i + lh$. As a result, the sampled information is transmitted and the triggering instant is updated to $t_{r+1}^i = t_r^i + lh$.

Remark 3. Owing to the fact that each triggering instant is selected from the sampling sequence, one has $\{t_0^i, t_1^i, t_2^i, \ldots\} \subseteq \{0, h, 2h, \ldots\}$. Hence, the inter-event intervals satisfy $t_{r+1}^i - t_r^i \geq h,\ (r = 0, 1, 2, \ldots)$. As a result, a strictly positive lower bound exists for every inter-event interval. By Definition 2.1, the proposed sampled-data event-triggered mechanism is therefore Zeno-free.

For convenience of subsequent analysis, define the piecewise-constant triggering error by $e_i(t) = e_i(s, t_r^i + lh),\ t \in [t_r^i + lh, t_r^i + (l+1)h)$.

By evaluating the triggering condition only at the sampling instants, the error signal is updated exclusively at these instants and remains unchanged between two consecutive sampling times. Therefore, for any $t \in [rh, (r+1)h)$, it follows that $e_i(t) = e_i(s, rh)$.

$$\begin{aligned}
\|e_i(s, t-\varsigma)\|_2 &\le \varphi_i \sum_{j\in\mathcal{N}_i} b_{ij} \left\|\tilde{z}_i\left(s, t_r^i\right) - \tilde{z}_j\left(s, t_{r'}^j\right)\right\|_2 \\
&\le \varphi_i \sum_{j\in\mathcal{N}_i} b_{ij} \left\|\tilde{z}_i(s, t-\varsigma) - \tilde{z}_j(s, t-\varsigma) + e_i(s, t-\varsigma) - e_j(s, t-\varsigma)\right\|_2 \\
&= \varphi_i \sum_{j\in\mathcal{N}_i} b_{ij} \left\|w_i(s, t-\varsigma) - w_j(s, t-\varsigma) + e_i(s, t-\varsigma) - e_j(s, t-\varsigma)\right\|_2 \\
&\le \varphi_i \sum_{j\in\mathcal{N}_i} b_{ij}\|w_i(s, t-\varsigma)\|_2 + \varphi_i \sum_{j\in\mathcal{N}_i} b_{ij}\|w_j(s, t-\varsigma)\|_2 + \varphi_i \sum_{j\in\mathcal{N}_i} b_{ij}\|e_i(s, t-\varsigma)\|_2 \\
&\quad + \varphi_i \sum_{j\in\mathcal{N}_i} b_{ij}\|e_j(s, t-\varsigma)\|_2 \\
&\le 2\varphi_i a\|w(s, t-\varsigma)\|_2 + 2\varphi_i a\|e(s, t-\varsigma)\|_2
\end{aligned} \tag{2.15}$$

Here, $e(s, t-\varsigma) = (e_1^{\mathrm{T}}(s, t-\varsigma), e_2^{\mathrm{T}}(s, t-\varsigma), \ldots, e_N^{\mathrm{T}}(s, t-\varsigma))^{\mathrm{T}}$, with $a = \max\left\{\sum_{j\in\mathcal{N}_i} b_{ij}\right\}$. Moreover, the final inequality in (2.15) follows from the Cauchy–Schwarz inequality.

Together with (2.15) and the norm properties, it follows that

$$\begin{aligned}
\|e(s, t-\varsigma)\|_2 &= \left(\sum_{i=1}^{N} \|e_i(s, t-\varsigma)\|_2^2\right)^{1/2} \\
&\le \left[\sum_{i=1}^{N} \left(2\varphi_i a\|w(s, t-\varsigma)\|_2 + 2\varphi_i a\|e(s, t-\varsigma)\|_2\right)^2\right]^{1/2} \\
&\le 2\varphi a\|w(s, t-\varsigma)\|_2 + 2\varphi a\|e(s, t-\varsigma)\|_2
\end{aligned} \tag{2.16}$$

Using (2.16), it can be derived that

$$\|e(s, t-\varsigma)\|_2 \le \frac{2\varphi a}{1-2\varphi a}\|w(s, t-\varsigma)\|_2 \tag{2.17}$$

with $0 < \varphi < \dfrac{1}{2a}$.

Definition 2.2 [2]. ES between Systems (2.1) and (2.4) is achieved if there exist constants $\epsilon > 0$ and $M > 1$ such that $\int_\Gamma \|v(s,t)\|_2^2\,\mathrm{d}s \le Me^{-\epsilon t}\int_\Gamma \|v(s,0)\|_2^2\,\mathrm{d}s$. Here, $v(s,t) = (v_1^{\mathrm{T}}(s,t), v_2^{\mathrm{T}}(s,t), \ldots, v_N^{\mathrm{T}}(s,t))^{\mathrm{T}} \in \mathbb{R}^{mN\times 1}$, where $s \in \Gamma$, and $v(s,0)$ denotes a bounded continuous initial function.

Definition 2.3 [5]. An asynchronous aperiodic intermittent controller is said to fulfill the average control ratio condition if there exist constants $\gamma_i \in (0,1)$ and $T_{\gamma_i} \ge 0$ such that $T_{\mathrm{con}}^i(t_1, t_2) \ge \gamma_i(t_1 - t_2) - T_{\gamma_i}$, $(\forall\, t_1 > t_2 \ge t_0)$, where $T_{\mathrm{con}}^i(t_1, t_2)$ denotes the total duration of the control-active intervals over $[t_2, t_1)$. The parameter γ_i is referred to as the asynchronous control ratio (ACR), whereas T_{γ_i} is termed the elasticity number.

Lemma 2.1 [4]: Assume that $n_o > 0$ $(o = 1, 2, \ldots, k)$. Let $\Gamma = \{s = (s_1, s_2, \ldots, s_k)^{\mathrm{T}} \mid \|s_o\|_2 < n_o,\ o = 1, 2, \ldots, k\}$ denote a hypercube in $\mathbb{R}^k$. Let $f(s)$ denote a continuously differentiable real-valued function in $C^1(\Gamma)$ that vanishes on the boundary $\partial\Gamma$ of Γ, that is, $f(s)|_{\partial\Gamma} = 0$. Then, it holds that

$$\int_\Gamma \phi^2(s)\,\mathrm{d}s \le n_o^2 \int_\Gamma \left\| \frac{\partial \phi(s)}{\partial s_o} \right\|_2^2 \mathrm{d}s.$$

Lemma 2.2 [15]: Let $N \geq 2$, and let ξ_i denote the cofactor of the i-th diagonal element of the Laplacian matrix associated with the directed graph $(\mathcal{G}, B)$, where $B = (b_{ij})_{N\times N}$. Then,

$$\sum_{i,j=1}^{N} \xi_i b_{ij} F_{ij}(v_i(s,t), v_j(s,t)) = \sum_{\delta\in\Gamma} W(\delta) \sum_{(x,r)\in E(C_\delta)} F_{rx}(v_r(s,t), v_x(s,t)).$$

Here, $F_{ij} : \mathbb{R}^m \times \mathbb{R}^m \to \mathbb{R}$, $i, j \in \mathcal{N}$, is an arbitrary real-valued function. Moreover, $W(\delta)$ denotes the weight associated with δ, C_δ denotes the directed cycle corresponding to δ, and Γ represents the collection of all spanning unicyclic subgraphs of the digraph $(\mathcal{G}, B)$. Furthermore, if $(\mathcal{G}, B)$ is strongly connected, then $\xi_i > 0$ holds for every $i \in \mathcal{N}$. Throughout this paper, the digraph $(\mathcal{G}, B)$ is assumed to be strongly connected.

Assumption 1. The vector-valued function $f_i(\cdot)$ satisfies

$$(w_i(s,t) - z_i(s,t))^{\mathrm{T}}(f_i(w_i(s,t)) - f_i(z_i(s,t))) \le \alpha_i (w_i(s,t) - z_i(s,t))^{\mathrm{T}}(w_i(s,t) - z_i(s,t)),$$

for some constant $\alpha_i > 0$.

Assumption 2. The coupling function $H_{ij}(\cdot,\cdot)$ satisfies

$$\|H_{ij}(s,y) - H_{ij}(\hat{s},\hat{y})\|_2 \le \delta_{ij}(\|s - \hat{s}\|_2 + \|y - \hat{y}\|_2),$$

for some constant $\delta_{ij} > 0$ and for all $s, \hat{s}, y, \hat{y} \in \mathbb{R}^m$.

Assumption 3. Under the specified initial and boundary conditions, the drive system (2.1) admits globally bounded solutions on $\Gamma \times [0, +\infty)$. In particular, there exists a positive constant M_z satisfying $\|z_i(s,t)\|_2 \le M_z$, for every $i \in \mathcal{N}$, $s \in \Gamma$, and $t \ge 0$.

Remark 4. The above assumptions are introduced to facilitate the synchronization analysis of reaction-diffusion neural networks and have clear physical meanings.

Assumption 1 imposes a one-sided Lipschitz condition on the activation functions, which is essential for estimating the nonlinear terms in the Lyapunov analysis.

Assumption 2 guarantees the boundedness of the coupling effects among interconnected nodes, allowing the synchronization criteria to be established for nonlinear network dynamics.

Assumption 3 ensures the global boundedness of the drive system states, which is necessary for obtaining finite estimates in the stability analysis and is consistent with the physical limitations of neural states.

These assumptions provide sufficient conditions for rigorous theoretical analysis while maintaining the applicability of the proposed method to a broad class of reaction-diffusion neural networks.

3. Results

3.1. Sufficient conditions for ES

Theorem 3.1 Suppose that Assumptions 1–3 hold. Define

$$\kappa^* = \min_i \left\{ \frac{2\lambda_{\min}(B_{io})}{n_o^2} - 2\alpha - 3\sum_j a_{ij}\delta_{ij} - \alpha(3+\varepsilon)\sum_j b_{ij} - 1 - \frac{\eta_{\max}}{\xi_{\min}} \right\}$$

where

$$\eta_{\max} = \max_i \left\{ \sum_k \xi_k (a_{ki}\delta_{ki} + \alpha b_{ki}) \right\}.$$

If $\kappa^* > 0$ and $h^2 - he^{-\mu h} + \frac{2\alpha h}{\varepsilon}\left(\sum_j b_{ij} + \frac{1}{\xi_i}\sum_j \xi_j b_{ji} \right) \leq 0$, then the drive system (2.1) and the response system (2.4) achieve ES for any $0 < \kappa < \kappa^*$.

The following corollaries follow directly from Theorem 3.1.

Corollary 3.1. Under the conditions of Theorem 3.1, the synchronization error converges exponentially with a convergence rate of at least $\rho + \kappa$, where

$$\rho = \min\{\kappa^* - \kappa, \delta, \mu\}.$$

Proof. The result follows directly from Theorem 3.1.

Corollary 3.2. Under the conditions of Theorem 3.1, any parameter satisfying

$$0 < \kappa < \kappa^*$$

guarantees ES of the considered reaction-diffusion neural networks.

Proof. The conclusion follows immediately from Theorem 3.1.

Proof. By Lemma 2.2, the strong connectivity of the digraph implies that $\xi_i > 0$ for all $i \in \mathcal{N}$. Accordingly, the following LKF is introduced:

$$V(t) = \sum_{i=1}^{N} \xi_i \left[V_{i1}(t) + V_{i2}(t) + V_{i3}(t) \right] \tag{3.1}$$

$$V_{i1}(t) = \int_\Gamma e^{\theta(t)} \|v_i(s,t)\|_2^2 \, ds, \tag{3.2}$$

$$V_{i2}(t) = \int_\Gamma \int_{t-h}^{t} e^{\delta(\tau - t)} \|v_i(s,\tau)\|_2^2 \, d\tau \, ds \tag{3.3}$$

$$V_{i3}(t) = h \int_\Gamma \int_{-h}^{0} \int_{t+\theta}^{t} e^{\mu(\tau - t)} \left\| \frac{\partial v_i(s,\tau)}{\partial \tau} \right\|_2^2 d\tau d\theta ds \tag{3.4}$$

From the choice $\theta(t) = \kappa t$ with a design constant $\kappa > 0$ follows continuous differentiability of $\theta(t)$ on $[0, +\infty)$ together with $\dot{\theta}(t) = \kappa$.The parameters $\delta > 0$ and $\mu > 0$ are design constants. They adjust the weights of historical states and state derivatives, respectively.

The time derivatives of $V_1(t)$, $V_2(t)$, and $V_3(t)$ are derived as

$$\dot{V}_{i1}(t) = \int_\Gamma e^{\theta(t)}\left[\kappa\|v_i\|_2^2 + 2v_i^T\frac{\partial v_i}{\partial t}\right]ds \tag{3.5}$$

$$\dot{V}_{i2} = \int_\Gamma \|v_i(t)\|_2^2 ds - e^{-\delta h}\int_\Gamma \|v_i(t-h)\|_2^2 ds - \delta V_{i2} \tag{3.6}$$

$$\dot{V}_{i3} \le h^2\int_\Gamma\left\|\frac{\partial v_i(t)}{\partial t}\right\|^2 ds \quad - he^{-\mu h}\int_\Gamma\int_{t-h}^t\left\|\frac{\partial v_i(\tau)}{\partial \tau}\right\|^2 d\tau ds \quad - \mu V_{i3} \tag{3.7}$$

By substituting (2.7) into (3.5), we obtain:

$$\begin{aligned}\dot{V}_{i1}(t) = \int_\Gamma e^{\theta(t)}\Big\{\kappa\|v_i\|_2^2 + 2v_i^{\mathrm{T}}\Big[\sum_{o=1}^k\frac{\partial}{\partial s_o}\Big(B_{io}\frac{\partial v_i}{\partial s_o}\Big) + f_i(w_i) - f_i(z_i)\\ + \sum_{j=1}^N a_{ij}(H_{ij}(w_i,w_j) - H_{ij}(z_i,z_j)) + u_i\Big]\Big\}ds\end{aligned} \tag{3.8}$$

Due to Lemma 2.1,we can get:

$$\int_\Gamma 2e^{\theta(t)}v_i^T\sum_o\frac{\partial}{\partial s_o}\left(B_{io}\frac{\partial v_i}{\partial s_o}\right)ds \le -\sum_o\frac{2\lambda_{\min}(B_{io})}{n_o^2}\int_\Gamma e^{\theta(t)}\|v_i\|_2^2 ds \tag{3.9}$$

$$2\int_\Gamma e^{\theta(t)}v_i^{\mathrm{T}}(f_i(w_i) - f_i(z_i))ds \le 2\alpha_i V_{i1} \tag{3.10}$$

By Assumption 2, the coupling functions satisfy the Lipschitz continuity condition. We get:

$$\begin{aligned}\left\|H_{ij}(w_i,w_j) - H_{ij}(z_i,z_j)\right\|_2 &\le \delta_{ij}(\|w_i - z_i\|_2 + \|w_j - z_j\|_2)\\ &= \delta_{ij}(\|v_i\|_2 + \|v_j\|_2).\end{aligned} \tag{3.11}$$

Then, according to the Cauchy–Schwarz inequality and Young's inequality, one obtains

$$\begin{aligned}2\int_\Gamma e^{\theta(t)}v_i^{\mathrm{T}}\sum_{j=1}^N a_{ij}(H_{ij}(w_i,w_j) - H_{ij}(z_i,z_j))ds &\le 2\sum_j a_{ij}\delta_{ij}\int_\Gamma e^{\theta(t)}(\|v_i\|^2 + \|v_i\|\|v_j\|)ds\\ &\le 3\left(\sum_j a_{ij}\delta_{ij}\right)V_{i1} + \sum_j a_{ij}\delta_{ij}\int_\Gamma e^{\theta(t)}\|v_j\|^2 ds\end{aligned} \tag{3.12}$$

Using the definitions of the triggering errors in (2.10)–(2.12), the sampled state difference can be decomposed as $\tilde{z}_i(s,t_r^i) - \tilde{z}_j(s,t_r^j) = [\tilde{z}_i(s,rh) - \tilde{z}_j(s,rh)] + [e_i(s,rh) - e_j(s,rh)]$.

Combining (2.10) with Jensen's inequality yields that$\|e_i(s,rh)\|^2 \le h\int_{rh-h}^{rh}\left\|\frac{\partial v_i(s,\tau)}{\partial\tau}\right\|^2 \mathrm{d}\tau$ and

$$
\begin{aligned}
2\int_\Gamma e^{\theta(t)} v_i^{\mathrm{T}} u_i \mathrm{d}s &= 2\alpha\int_\Gamma e^{\theta(t)} v_i^{\mathrm{T}} \sum_j b_{ij}[(v_i - v_j) + (e_i - e_j)]\mathrm{d}s \\
&= 2\alpha\sum_j b_{ij}\int_\Gamma e^{\theta(t)} v_i^{\mathrm{T}}(v_i - v_j)\mathrm{d}s + 2\alpha\sum_j b_{ij}\int_\Gamma e^{\theta(t)} v_i^{\mathrm{T}}(e_i - e_j)\mathrm{d}s \\
&\le 3\alpha\left(\sum_j b_{ij}\right)V_{i1} + \alpha\sum_j b_{ij}\int_\Gamma e^{\theta(t)}\|v_j\|^2\mathrm{d}s + \alpha\varepsilon\left(\sum_j b_{ij}\right)V_{i1} + \frac{\alpha}{\varepsilon}\sum_j b_{ij}\int_\Gamma e^{\theta(t)}\|e_i - e_j\|^2\mathrm{d}s \\
&\le \alpha(3+\varepsilon)\left(\sum_j b_{ij}\right)V_{i1} + \alpha\sum_j b_{ij}\int_\Gamma e^{\theta(t)}\|v_j\|^2\mathrm{d}s + \frac{2\alpha}{\varepsilon}\sum_j b_{ij}\int_\Gamma e^{\theta(t)}(\|e_i\|^2 + \|e_j\|^2)\mathrm{d}s \\
&\le \alpha(3+\varepsilon)\left(\sum_j b_{ij}\right)V_{i1} + \alpha\sum_j b_{ij}\int_\Gamma e^{\theta(t)}\|v_j\|^2\mathrm{d}s \\
&\quad + \frac{2\alpha h}{\varepsilon}\sum_j b_{ij}\int_\Gamma e^{\theta(t)}\int_{rh-h}^{rh}\left(\left\|\frac{\partial v_i}{\partial\tau}\right\|^2 + \left\|\frac{\partial v_j}{\partial\tau}\right\|^2\right)\mathrm{d}\tau\mathrm{d}s.
\end{aligned}
\tag{3.13}
$$

From substituting (3.10)–(3.13) into (3.9) follows the final expression:

$$
\begin{aligned}
\dot V_{i1} \le &\left[\kappa - \frac{2\lambda_{\min}(B_{io})}{n_o^2} + 2\alpha + 3\sum_{j=1}^N a_{ij}\delta_{ij} + \alpha(3+\varepsilon)\sum_{j=1}^N b_{ij}\right]V_{i1} + \sum_{j=1}^N(a_{ij}\delta_{ij} + \alpha b_{ij})\int_\Gamma e^{\theta(t)}\|v_j\|^2 ds \\
&+ \frac{2\alpha h}{\varepsilon}\sum_{j=1}^N b_{ij}\int_\Gamma e^{\theta(t)}\int_{rh-h}^{rh}(\|\dot v_i(\tau)\|^2 + \|\dot v_j(\tau)\|^2)d\tau ds
\end{aligned}
\tag{3.14}
$$

since $rh \le t < (r+1)h$,$\int_{rh-h}^{rh}\left\|\frac{\partial v_i}{\partial\tau}\right\|^2\mathrm{d}\tau \le \int_{t-h}^{t}\left\|\frac{\partial v_i}{\partial\tau}\right\|^2\mathrm{d}\tau$.

Let $\xi = (\xi_1,\ldots,\xi_N)^{\mathrm{T}}$ be the positive left eigenvector associated with the zero eigenvalue of the Laplacian matrix L (Lemma 2.2).

Unlike LKFs for continuous or periodically sampled control systems, the proposed functional is designed for the sampled-data event-triggered asynchronous intermittent control protocol and captures the effects of sampled-data communication and intermittent control through state, historical-state, and state-derivative terms.

Then, define the global Lyapunov functional

$$
\dot V(t) = \sum_{i=1}^N \xi_i\left[\dot V_{i1}(t) + \dot V_{i2}(t) + \dot V_{i3}(t)\right] \tag{3.15}
$$

Substituting (3.14) into (3.15) yields

$$\sum_i \xi_i \dot{V}_{i1} \leq \sum_i \xi_i \left[\kappa - \frac{2\lambda_{\min}(B_{io})}{n_o^2} + 2\alpha + 3\sum_j a_{ij}\delta_{ij} + \alpha(3+\varepsilon)\sum_j b_{ij} \right] V_{i1}$$
$$+ \sum_i \xi_i \sum_j (a_{ij}\delta_{ij} + \alpha b_{ij}) \int_\Gamma e^{\theta} \|v_j\|^2 ds \quad + \frac{2\alpha h}{\varepsilon} \sum_i \xi_i \sum_j b_{ij} \int_\Gamma e^{\theta} \int_{t-h}^{t} (\|\dot{v}_i\|^2 + \|\dot{v}_j\|^2) d\tau ds \tag{3.16}$$

$$\sum_i \xi_i \dot{V}_{i2} = \sum_i \xi_i e^{-\kappa t} V_{i1} - e^{-\delta h} \sum_i \xi_i \int_\Gamma \|v_i(t-h)\|^2 ds \quad - \delta \sum_i \xi_i V_{i2}. \tag{3.17}$$

$$\sum_i \xi_i \dot{V}_{i3} \leq h^2 \sum_i \xi_i \int_\Gamma \int_{t-h}^{t} \|\dot{v}_i\|^2 \mathrm{d}\tau \mathrm{d}s - he^{-\mu h} \sum_i \xi_i \int_\Gamma \int_{t-h}^{t} \|\dot{v}_i(\tau)\|^2 d\tau ds \quad - \mu \sum_i \xi_i V_{i3} \tag{3.18}$$

Combining partial terms in (3.16)–(3.18) leads to

$$\frac{2\alpha h}{\varepsilon} \sum_i \xi_i \sum_j b_{ij} \int_\Gamma e^{\theta(t)} \int_{rh-h}^{rh} (\|\dot{v}_i\|^2 + \|\dot{v}_j\|^2) \mathrm{d}\tau \mathrm{d}s \leq \frac{2\alpha h}{\varepsilon} \sum_i \xi_i \sum_j b_{ij} \int_\Gamma \int_{t-h}^{t} (\|\dot{v}_i(\tau)\|^2 + \|\dot{v}_j(\tau)\|^2) \mathrm{d}\tau \mathrm{d}s \tag{3.19}$$

$$h^2 \sum_i \xi_i \int_\Gamma \int_{t-h}^{t} \|\dot{v}_i\|^2 \mathrm{d}\tau \mathrm{d}s + \frac{2\alpha h}{\varepsilon} \sum_i \xi_i \sum_j b_{ij} \int_\Gamma \int_{t-h}^{t} \|\dot{v}_i\|^2 \mathrm{d}\tau \mathrm{d}s$$
$$+ \frac{2\alpha h}{\varepsilon} \sum_j \Big(\sum_i \xi_i b_{ij} \Big) \int_\Gamma \int_{t-h}^{t} \|\dot{v}_j\|^2 \mathrm{d}\tau \mathrm{d}s - he^{-\mu h} \sum_i \xi_i \int_\Gamma \int_{t-h}^{t} \|\dot{v}_i\|^2 \mathrm{d}\tau \mathrm{d}s$$
$$\leq \sum_i \xi_i \int_\Gamma \int_{t-h}^{t} \left[\left(h^2 - he^{-\mu h} + \frac{2\alpha h}{\varepsilon} \sum_j b_{ij} \right) \|\dot{v}_i\|^2 \right] \mathrm{d}\tau \mathrm{d}s + \frac{2\alpha h}{\varepsilon} \sum_j \Big(\sum_i \xi_i b_{ij} \Big) \int_\Gamma \int_{t-h}^{t} \|\dot{v}_j\|^2 \mathrm{d}\tau \mathrm{d}s$$
$$\leq \sum_i \int_\Gamma \int_{t-h}^{t} \left\{ \xi_i \left(h^2 - he^{-\mu h} + \frac{2\alpha h}{\varepsilon} \sum_j b_{ij} \right) + \frac{2\alpha h}{\varepsilon} \left(\sum_j \xi_j b_{ji} \right) \right\} \|\dot{v}_i\|^2 \mathrm{d}\tau \mathrm{d}s \tag{3.20}$$

By choosing $h^2 - he^{-\mu h} + \frac{2\alpha h}{\varepsilon} \left(\sum_j b_{ij} + \frac{1}{\xi_i} \sum_j \xi_j b_{ji} \right) \leq 0$, the integral term in (3.19) is nonpositive and can therefore be discarded.

$$\sum_{i=1}^{N} \xi_i \sum_{j=1}^{N} (a_{ij}\delta_{ij} + \alpha b_{ij}) \int_\Gamma e^{\theta(t)} \|v_j(s,t)\|^2 ds = \sum_{j=1}^{N} \left(\sum_{i=1}^{N} \xi_i (a_{ij}\delta_{ij} + \alpha b_{ij}) \right) \int_\Gamma e^{\theta(t)} \|v_j(s,t)\|^2 ds. \tag{3.21}$$

Let $\eta_i = \sum_k \xi_k (a_{ki}\delta_{ki} + \alpha b_{ki})$ and $\eta_i \leq \eta_{\max} = \max_i \eta_i$, $\xi_{\min} = \min_i \xi_i > 0$. Then we arrive at $\sum_i \xi_i \sum_j (a_{ij}\delta_{ij} + \alpha b_{ij}) \int_\Gamma e^{\theta} \|v_j\|^2 \mathrm{d}s = \sum_i \eta_i \int_\Gamma e^{\theta} \|v_i\|^2 \mathrm{d}s = \sum_i \eta_i V_{i1} \leq \eta_{\max} \sum_i V_{i1} \leq \frac{\eta_{\max}}{\xi_{\min}} \sum_i \xi_i V_{i1}$.

Substituting (3.16)–(3.21) into (3.15), we obtain:

$$\dot{V}(t) \leq \sum_{i=1}^{N} \left[\kappa - \frac{2\lambda_{\min}(B_{io})}{n_o^2} + 2\alpha + 3\sum_j a_{ij}\delta_{ij} + \alpha(3+\varepsilon)\sum_j b_{ij} + 1 + \frac{\eta_{\max}}{\xi_{\min}} \right] \xi_i V_{i1}$$
$$- \delta \sum_i \xi_i V_{i2} - \mu \sum_i \xi_i V_{i3} \tag{3.22}$$

By introducing the following parameters:

$$\kappa^* = \min_i \left\{ \frac{2\lambda_{\min}(B_{io})}{n_o^2} - 2\alpha - 3\sum_j a_{ij}\delta_{ij} - \alpha(3+\varepsilon)\sum_j b_{ij} - 1 - \frac{\eta_{\max}}{\xi_{\min}} \right\} \tag{3.23}$$

Then choose a design parameter κ satisfying $0 < \kappa < \kappa^*$.

The condition (3.23) can be further rewritten as

$$\dot{V}(t) \leq -(\kappa^* - \kappa)\sum_i \xi_i V_{i1} - \delta \sum_i \xi_i V_{i2} - \mu \sum_i \xi_i V_{i3}. \tag{3.24}$$

Since $\kappa^* > 0$ and $0 < \kappa < \kappa^*$, one has $\kappa^* - \kappa > 0$. Together with $\delta > 0$ and $\mu > 0$, define $\rho = \min\{\kappa^* - \kappa, \delta, \mu\} > 0$.

Consequently,

$$\dot{V}(t) \leq -\rho \sum_{i=1}^{N} \xi_i \left(V_{i1}(t) + V_{i2}(t) + V_{i3}(t)\right) = -\rho V(t). \tag{3.25}$$

Then by the comparison principle,

$$V(t) \leq V(0)e^{-\rho t}. \tag{3.26}$$

Since $V_{i2}(t) \geq 0$, $V_{i3}(t) \geq 0$, one has $V(t) \geq \sum_{i=1}^{N} \xi_i V_{i1}(t)$. Let $\xi_{\min} = \min_{1\leq i\leq N} \xi_i$, therefore, $V(t) \geq e^{\kappa t}\sum_{i=1}^{N} \xi_i \int_\Gamma \|v_i(s,t)\|^2 ds$.Then$V(t) \geq \xi_{\min} e^{\kappa t} \int_\Gamma \|v(s,t)\|^2 ds$, and we obtain

$$\xi_{\min} e^{\kappa t} \int_\Gamma \|v(s,t)\|^2 ds \leq V(0)e^{-\rho t}. \tag{3.27}$$

That is, $\int_\Gamma \|v(s,t)\|^2 ds \leq \frac{V(0)}{\xi_{\min}} e^{-(\rho+\kappa)t}$. $V(0) \leq M_0 \int_\Gamma \|v(s,0)\|^2 ds$ for some constant $M_0 > 0$.

Then, $\int_\Gamma \|v(s,t)\|^2 ds \leq \frac{M_0}{\xi_{\min}} e^{-(\rho+\kappa)t} \int_\Gamma \|v(s,0)\|^2 ds$. Therefore, by Definition 2.2, the drive system is exponentially synchronized with the response system.

4. Simulation results

To illustrate the effectiveness of the proposed sampled-data event-triggered asynchronous aperiodic intermittent control scheme and verify the theoretical results in Section 3, numerical simulations are conducted. First, a four-node reaction-diffusion neural network is considered to demonstrate the synchronization performance. Moreover, a 16-node network is further introduced to evaluate the scalability and communication efficiency of the proposed method.

For the four-node network, the communication topology is described by the directed adjacency matrix

$$G = \begin{bmatrix} 0 & 1 & 0 & 0 \\ 0 & 0 & 0 & 1 \\ 1 & 0 & 0 & 0 \\ 1 & 0 & 1 & 0 \end{bmatrix}.$$

The spatial domain is selected as $\Gamma = (-0.5, 0.5)$ with homogeneous Dirichlet boundary conditions. The spatial interval is discretized into $N = 80$ grid points with $ds \approx 0.0127$. The simulation time and integration step are set as $t = 10$ and $\Delta t = 0.0005$, respectively. The system parameters are selected as $k = [1.50, 1.30, 1.20, 1.10]$, $c = [6.0, 5.5, 5.0, 5.0]$, and $\alpha = 0.6$. The nonlinear activation function is given by $f(x) = \frac{|x+1|-|x-1|}{2}$.

4.1. Synchronization performance

Figure 1 illustrates the spatiotemporal evolutions of the drive and response systems. The four subfigures correspond to z_1, w_1, z_2, and w_2, respectively. Although different initial conditions are considered, the response systems gradually converge to the drive systems, indicating successful synchronization under the proposed controller.

Figure 2 shows the synchronization error under the typical threshold $\phi = 0.05$. The error decreases exponentially and exhibits an approximately linear trend in the semilogarithmic scale, which verifies the exponential convergence property established in Theorem 3.1.

4.2. Threshold sensitivity analysis

To investigate the influence of the triggering threshold amplitude ϕ, four different values are considered: $\phi \in \{0.02, 0.05, 0.20, 0.60\}$.

The triggering threshold φ governs the trade-off between synchronization performance and communication efficiency. A smaller value of φ yields more frequent triggering instants and faster convergence of synchronization errors, whereas a larger φ decreases the frequency of communication updates yet may degrade the synchronization rate. Moreover, since triggering instants are confined to the sampling time sequence, the proposed strategy ensures a strictly positive minimum inter-event interval, thereby eliminating Zeno behavior.

Figure 3 compares the synchronization errors and triggering characteristics under different threshold values. Smaller thresholds provide faster convergence and lower synchronization errors, while larger thresholds reduce triggering events at the cost of slower convergence. This result reveals the trade-off between communication efficiency and synchronization performance.

4.3. Scalability and communication efficiency comparison

To further evaluate the scalability and effectiveness of the proposed method, a 16-node reaction-diffusion neural network is considered. The proposed scheme is compared with continuous control and periodic sampled-data control schemes in terms of synchronization performance and communication efficiency.

Figure 4 presents the synchronization performance comparison among the three control strategies. All methods successfully achieve synchronization, demonstrating their effectiveness in stabilizing the network. However, compared with continuous and periodic sampled-data control schemes, the proposed event-triggered strategy achieves comparable convergence performance with fewer communication updates, which highlights its advantage in reducing unnecessary information exchange.

Figure 5 depicts the number of triggering events for each node under the proposed control scheme. The limited triggering frequency demonstrates that the proposed strategy reduces communication transmissions while preserving synchronization performance in larger-scale networks.

The communication saving ratio is calculated as $R_s = \frac{N_{\text{baseline}} - N_{\text{proposed}}}{N_{\text{baseline}}} \times 100\%$.

The comparison results indicate that the proposed method can significantly reduce communication overhead while preserving desired synchronization performance, demonstrating its potential for communication-efficient synchronization of large-scale reaction-diffusion neural networks.

4.4. Discussion and consistency with theoretical results

The simulation results are consistent with the theoretical conclusions in Section 3. Figures 1 and 2 verify the synchronization capability and exponential convergence property of the proposed controller. Figure 3 demonstrates the influence of the triggering threshold on synchronization performance and communication efficiency. Furthermore, Figures 4 and 5 illustrate that the proposed strategy maintains synchronization performance while reducing communication updates in larger-scale networks.

Therefore, the proposed sampled-data event-triggered asynchronous aperiodic intermittent control scheme provides an effective and communication-efficient solution for synchronization of reaction-diffusion neural networks.

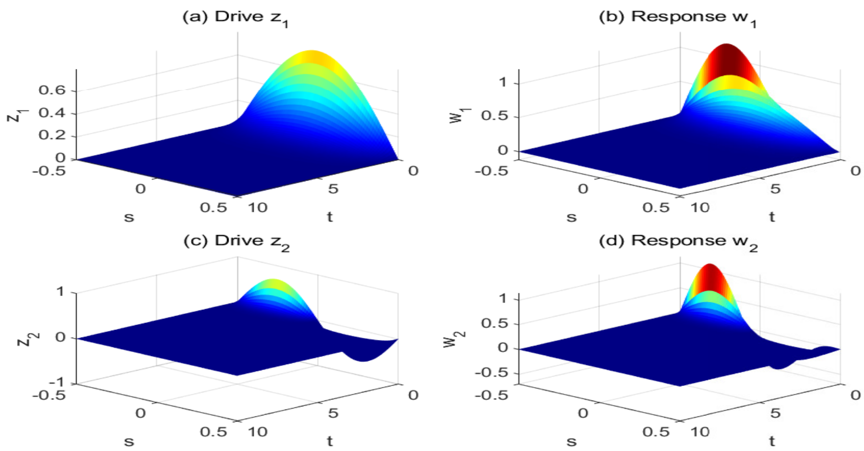

Figure 1. Spatiotemporal state evolutions of the drive and response systems.

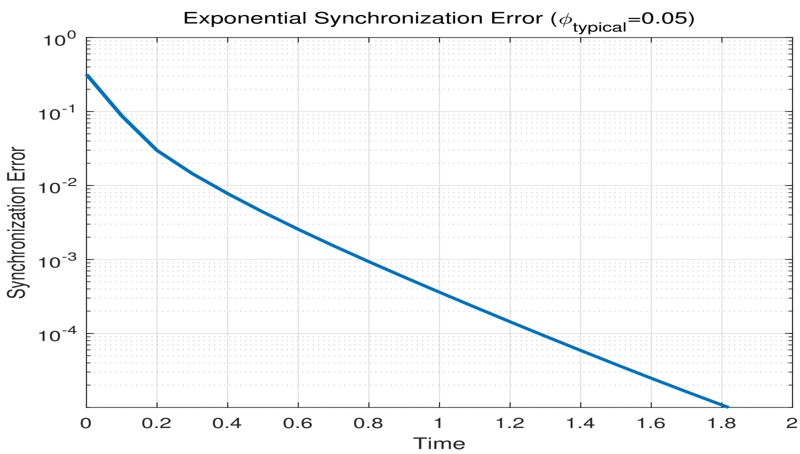

Figure 2. ES error under a typical triggering threshold $\phi = 0.05$.

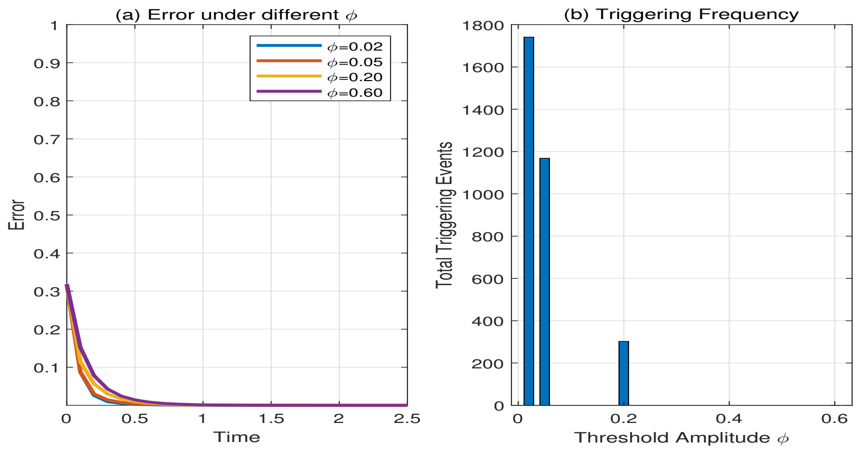

Figure 3. Effects of threshold amplitude on synchronization performance and triggering events.

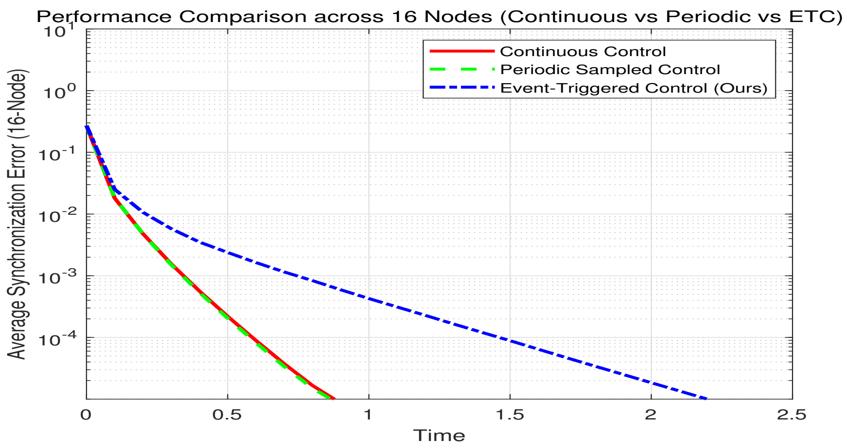

Figure 4. Comparison of synchronization performance among different control schemes.

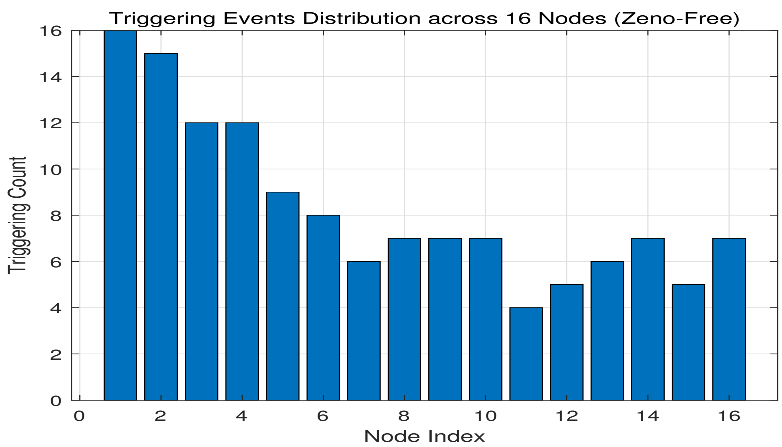

Figure 5. Triggering events of different nodes under event-triggered control.

5. Conclusions

In this paper, a sampled-data event-triggered asynchronous aperiodic intermittent control strategy has been developed for the ES of reaction-diffusion neural networks over directed topologies. By constructing an LKF and utilizing graph-theoretic techniques, sufficient synchronization conditions have been established, and the Zeno-free property of the proposed scheme has been verified.

Numerical results demonstrate that the proposed method achieves synchronization while reducing communication transmissions. The threshold analysis further illustrates the trade-off between synchronization performance and communication efficiency, confirming the effectiveness of the proposed control strategy.

Future research will focus on extending the proposed framework to finite-time and fixed-time synchronization problems, as well as investigating more practical scenarios involving model uncertainties, communication delays, and switching topologies.

Use of AI tools declaration

All research content, academic viewpoints, data arguments, and core conclusions presented in this paper were independently completed by the authors. AI tools served only as auxiliary means and did not participate in core academic processes such as research design, data processing, or conclusion derivation. The authors strictly adhered to academic integrity norms and the relevant requirements of the journal.

Conflict of interest

The authors declare there are no conflicts of interest.

References

1. H. Zeng, G. Chen, X. Wang, Observer-based event-triggered scheme for finite-time control of discrete-time linear time-varying networked control systems, *J. Nonlinear Dyn. Appl.*, **2** (2026), 108–118. https://doi.org/10.62762/JNDA.2026.314876
2. D. V. Dimarogonas, E. Frazzoli, K. H. Johansson, Distributed event-triggered control for multi-agent systems, *IEEE Trans. Autom. Control*, **57** (2012), 1291–1297. https://doi.org/10.1109/TAC.2011.2174666
3. A. Girard, Dynamic triggering mechanisms for event-triggered control, *IEEE Trans. Autom. Control*, **60** (2015), 1992–1997. https://doi.org/10.1109/TAC.2014.2366855
4. J. G. Lu, Global exponential stability and periodicity of reaction–diffusion delayed recurrent neural networks with Dirichlet boundary conditions, *Chaos Solitons Fractals*, **35** (2008), 116–125. https://doi.org/10.1016/j.chaos.2007.05.002
5. G. Zhang, J. Hu, S. Wen, New results on fixed/preassigned-time stabilization of the discontinuous neural networks with mixed time-varying delays, *Neurocomputing*, **682** (2026), 133464. https://doi.org/10.1016/j.neucom.2026.133464
6. Y. Wu, Z. Sun, G. Ran, L. Xue, Intermittent control for fixed-time synchronization of coupled networks, *IEEE/CAA J. Autom. Sin.*, **10** (2023), 1488–1490. https://doi.org/10.1109/JAS.2023.123363

7. Y. Huang, S. Lin, E. Yang, Event-triggered passivity of multi-weighted coupled delayed reaction–diffusion memristive neural networks with fixed and switching topologies, *Commun. Nonlinear Sci. Numer. Simul.*, **89** (2020), 1–28. https://doi.org/10.1016/j.cnsns.2020.105292

8. X. M. Zhang, Q. L. Han, B. Zhang, X. Ge, Monotonically-increasing-function-based event-triggered sampling scheme for stabilization of networked nonlinear systems, *Sci. China Inf. Sci.*, **69** (2026), 152201. https://doi.org/10.1007/s11432-025-4644-x

9. X. M. Zhang, Q. L. Han, B. L. Zhang, X. Ge, D. Zhang, Accumulated-state-error-based event-triggered sampling scheme and its application to H_∞ control of sampled-data systems, *Sci. China Inf. Sci.*, **67** (2024), 162206. https://doi.org/10.1007/s11432-023-4038-3

10. C. Huang, W. Wang, J. Cao, J. Lu, Synchronization-based passivity of partially coupled neural networks with event-triggered communication, *Neurocomputing*, **319** (2018), 134–143. https://doi.org/10.1016/j.neucom.2018.08.060

11. X. Ma, B. Liu, X. Jia, X. M. Zhang, Synchronization control of chaotic neural networks subject to actuator saturation under event-triggered sampling scheme, *Neurocomputing*, **677** (2026), 133038. https://doi.org/10.1016/j.neucom.2026.133038

12. S. Lin, Y. Huang, S. Ren, Event-triggered passivity and synchronization of delayed multiple-weighted coupled reaction–diffusion neural networks with non-identical nodes, *Neural Networks*, **121** (2020), 259–275. https://doi.org/10.1016/j.neunet.2019.08.031

13. Q. Qiu, H. Su, Sampling-based event-triggered exponential synchronization for reaction–diffusion neural networks, *IEEE Trans. Neural Networks Learn. Syst.*, **34** (2023), 1209–1217. https://doi.org/10.1109/TNNLS.2021.3105126

14. J. Liu, Y. Yang, Y. Wu, S. Al-Dabooni, L. Xue, D. C. Wunsch, Exponential synchronization of reaction–diffusion systems on networks via asynchronous intermittent control, *IEEE Trans. Signal Inf. Process. Networks*, **9** (2023), 825–834. https://doi.org/10.1109/TSIPN.2023.3338452

15. B. Zhou, X. Liao, T. Huang, Event-based exponential synchronization of complex networks, *Cogn. Neurodyn.*, **10** (2016), 423–436. https://doi.org/10.1007/s11571-016-9391-3

AIMS Press